



Research Article

Clinicopathologic and Genomic Characteristics of Minute Pulmonary Meningothelial-like Nodules

Haochen Li^{a,b}, Zhicheng Huang^a, Yadong Wang^a, Chao Guo^a, Xiaoyu Li^c, Weixun Zhou^c, Sha Wang^d, Na Bai^d, Hanlin Chen^d, Bowen Li^a, Daoyun Wang^a, Zhibo Zheng^{a,e}, Zhongxing Bing^a, Yang Song^a, Yuan Xu^a, Guanghua Huang^a, Ka Luk Fung^f, Lan Song^g, Naixin Liang^{a,*}, Shanqing Li^{a,*}

^a Department of Thoracic Surgery, Peking Union Medical College Hospital, Chinese Academy of Medical Sciences and Peking Union Medical College, Beijing, China; ^b School of Medicine, Tsinghua Medicine, Tsinghua University, Beijing, China; ^c Department of Pathology, Peking Union Medical College Hospital, Chinese Academy of Medical Sciences and Peking Union Medical College, Beijing, China; ^d Geneseeq Research Institute, Geneseeq Technology Inc, Nanjing, China; ^e Department of International Medical Services, Peking Union Medical College Hospital, Chinese Academy of Medical Sciences, Beijing, China; ^f University of Toronto, Toronto, Canada; ^g Department of Radiology, Peking Union Medical College Hospital, Chinese Academy of Medical Sciences and Peking Union Medical College, Beijing, China

ARTICLE INFO

Article history:

Received 1 October 2024

Revised 24 March 2025

Accepted 23 April 2025

Available online 29 April 2025

Keywords:

minute pulmonary meningothelial-like nodule
whole-exome sequencing
immunohistochemistry
radiology
reactive hyperplasia

ABSTRACT

Minute pulmonary meningothelial-like nodules (MPMNs) are benign lung lesions with histologic characteristics similar to meningeal epithelium. MPMNs often lead to misdiagnosis for their similar radiologic characteristics to malignant nodules. The pathogenesis of MPMNs remains unclear, and this research primarily focused on mutations in a limited number of genes, lacking a comprehensive analysis of their mutational landscape. We collected 134 MPMNs from 88 patients with pathologic examinations at Peking Union Medical College Hospital in the past 5 years. We performed whole-exome sequencing on 12 MPMNs and 7 adenocarcinoma lesions from 6 patients. In our PUMCH-MPMN cohort, we provided clinical, pathologic, radiologic, and follow-up characteristics of patients with MPMNs. Our study demonstrated the pathologic diagnostic value of 3 classic MPMN diagnostic markers (epithelial membrane antigen, progesterone receptor, and vimentin) and the novel marker somatostatin receptor 2. It also suggested the preoperative differential diagnostic value of positron emission tomography/computed tomography. We also classified MPMNs into 4 types based on different discovery methods and verified the diagnostic value of traditional and novel immunohistochemical markers. We performed whole-exome sequencing and revealed that MPMNs harbor mutations enriched in cell cycle and cytoskeleton assembly pathways. On the other hand, classical meningioma-related mutations, such as *NF2* mutations, were not detected. These findings provide new evidence for the hypothesis that MPMNs arise from reactive proliferation rather than share a common origin with meningiomas, contributing to a better understanding of MPMNs among clinicians and pathologists, reducing misdiagnosis, and improving patient care.

© 2025 United States & Canadian Academy of Pathology. Published by Elsevier Inc. All rights are reserved, including those for text and data mining, AI training, and similar technologies.

* These authors contributed equally: Haochen Li and Zhicheng Huang.

* Corresponding authors.

E-mail addresses: pumchnelson@163.com, liangnaixin@pumch.cn (N. Liang), lishanqing@pumch.cn (S. Li).



Introduction

Minute pulmonary meningotheelial-like nodules (MPMNPs) are a type of benign lesions in the lungs, named for their similar histologic features and immunohistochemical (IHC) characteristics to the meningeal epithelium. In 1960, Korn et al¹ first named these lesions pulmonary chemodectoma. Gaffey et al² later found that MPMNPs are similar to meningeal epithelial cells and contain no endocrine granules. Thus, they renamed them meningeal epithelioid nodules.^{2,3} On computed tomography (CT) imaging, MPMNPs typically present as pure ground-glass opacities (GGOs), with some mimicking malignant nodules. It is challenging to distinguish MPMNPs from malignant nodules based on CT images, which can lead to misdiagnosis in clinical practice.⁴ According to the 11th edition of *Rosai and Ackerman's Surgical Pathology*,⁵ the diagnostic criteria for MPMNPs are established based on histologic and immunohistochemical features (positive for vimentin, epithelial membrane antigen [EMA], and creatine kinase and negative for neuroendocrine and melanoma markers), combined with macroscopic and ultrastructural characteristics.

In recent years, studies have reported the typical characteristics and some rare manifestations of MPMNPs,^{6–11} but there is currently no clear consensus on the pathogenesis of MPMNPs.¹² On the one hand, according to autopsy and surgical lung resection samples, MPMNPs are more common in patients with chronic lung diseases such as tumors, thromboembolic diseases, and infarcts, and have not been reported in children. These epidemiologic characteristics of MPMNPs indicate that the generation of MPMNPs is a chronic process with the influence of other diseases.¹³ On the other hand, some studies suggest the formation and progression of MPMNPs depend on similar molecular pathways to meningiomas, according to their similar histologic characteristics and common genomic variations.^{11,14} However, previous studies have largely relied on fluorescence in situ hybridization to analyze a limited number of genes, leaving the comprehensive mutational landscape of MPMNPs unexplored and limiting the understanding of their molecular etiology.

Beyond pathogenesis, the clinical characteristics of MPMNPs remain a subject of debate. Historically, MPMNPs have been identified through targeted examinations of excised tissue, predominantly as nonindependent lesions adjacent to tumors.^{13,15} However, with the increasing use of low-dose CT screening for lung cancer and the growing recognition of multiple primary lung cancers (MPLCs), more independent MPMNPs are being detected and misdiagnosed as MPLC lesions, leading to unnecessary surgical interventions and increased patient burden. This underscores the need to reassess the clinical, radiologic, and pathologic features of MPMNPs, differentiate independent from nonindependent MPMNPs, and establish a classification system for their clinical presentation.

In this study, our PUMCH-MPMN cohort enrolled 88 patients with 134 MPMNPs in total from patients who underwent pathologic examinations at Peking Union Medical College Hospital from April 2019 to April 2024. Based on our cohort (PUMCH-MPMN), we collected the clinical, pathologic, radiologic, and follow-up characteristics of MPMNPs and summarized different clinical pathways for finding these MPMNPs. Furthermore, we performed whole-exome sequencing (WES) on 12 MPMNPs and 7 adenocarcinoma lesions from 6 patients in our cohort. We obtained the comprehensive mutation profiles of MPMNPs and conducted a comparison with multiple primary malignant lesions in these patients. To the best of our knowledge, our study is the first research to detect the WES results of MPMNPs and explore the clinical characteristics of MPMNPs in the context of increasingly popular MPLCs. Our findings provide

novel evidence and insights into MPMNPs, offering valuable guidance to surgeons and pathologists in understanding and accurately diagnosing MPMNPs, minimizing misdiagnosis, and ultimately relieving the suffering of patients.

Materials and Methods

Patients and Sample Details

We retrospectively analyzed patients who underwent pathologic examinations at Peking Union Medical College Hospital from April 2019 to April 2024. According to Gaffey's criteria and *Rosai and Ackerman's Surgical Pathology*,^{2,5} 88 patients and 134 MPMNPs met the diagnostic criteria. Of the 88 patients, 69 underwent surgery at Peking Union Medical College Hospital. The remaining patients underwent surgery in external hospitals and presented their excised samples to our outpatient department. We collected clinical and radiologic information from these patients.

We collected samples and performed WES on 12 MPMNPs and 7 lung tumors from 6 patients. This study involved human participants and was approved by the ethical committee of Peking Union Medical College Hospital (K7403). All patients signed written informed consent forms for genomic profiling.

Whole-Exome Library Preparation and Sequencing

Genomic DNA from formalin-fixed and paraffin-embedded samples was extracted using QIAamp DNA FFPE Tissue Kit (Qia-Gen) and fragmented by M220 Focused-ultrasonicator (Covaris) into ~250 bp. According to the manufacturer's protocol, a whole-genome library was prepared using the KAPA Hyper Prep Kit (KAPAxGen Exome Hybridization Panel; Integrated DNA Technologies Inc). Captured libraries were amplified in KAPA HiFi HotStart ReadyMix (KAPA Biosystems) and purified using Agen-court AMPure XP beads. Enriched libraries were sequenced using the Illumina HiSeq 4000 platform as paired 125-bp reads according to the manufacturer's instructions.

Variant Filtering and Mutation Calling

The sequence data were processed as previously described.¹⁶ For quality control procedures, Trimmomatic was used to remove low-quality samples (quality reading below 20) or N bases from the FASTQ files. Sequencing reads were mapped to the reference human genome (hg19) using the Sentieon. Sentieon software removed duplicate reads, followed by realignment around known insertion/deletions (indels). Base quality recalibration was performed using GATK4, and samples with Total QScores <35 or contamination rates >0.02 were excluded. Fingerprint was used to remove nonmatching samples from matched tumor–normal pairs. GATK4 was used to estimate cross-sample contamination. Somatic single nucleotide variant (SNV) calling and indels calling were performed using Vardict.¹⁷ SNV in the 1000 Genomes Project and dbSNP with frequency of >1% were excluded. The SNVs and indels were further filtered as previously described.¹⁶

Pathway Analysis

We performed functional enrichment analyses using Kyoto Encyclopedia of Genes and Genomes and Gene Ontology

databases to examine the biological functions of the most frequently mutated genes. Pathways with *P* values of <.05 and Benjamini–Hochberg adjusted *P* values of <.1 were displayed.

Reconstruction of Clonal and Subclonal Architecture and Tumor Evolution

Pyclone was used to estimate significant clones and subclones and reconstruct the phylogenetic tree. Cellular prevalence was estimated based on allele frequency and copy numbers to adjust for tumor purities and was used for mutation clustering. For each dissected or single tumor region, mutations with ccf of >0.6 were considered as clonal events and otherwise subclonal. SCHISM¹⁸ was then used to reconstruct clonal and subclonal hierarchies.

Statistical Analysis

Descriptive statistics were used to summarize the demographic, clinical, and imaging characteristics of the cohort. Continuous variables (such as age and nodule diameter) were expressed as means, and categorical variables (such as sex, smoking history, and imaging characteristics) were reported as frequencies and percentages. The lobular and lateral distribution preferences of MPMNs were analyzed using the 1-sample proportion z-test, and a comparison of continuous variables between 2 groups was performed using the Wilcoxon rank sum test. Statistical significance was defined as a test *P* value of <.05. Statistical analysis was conducted using the R language.

Immunohistochemistry Staining

IHC staining followed standard procedures: (1) washing using buffer and preprocess; (2) blocking endogenous peroxidase: FLEX Peroxidase Block for 5 minutes; and (3) adding the primary antibody and incubating in a wet box. The primary antibodies against EMA (41617395; Agilent; incubation for 20 minutes), S-100 (41651587; Agilent; incubation for 30 minutes), vimentin (41727949; Agilent; incubation for 30 minutes), somatostatin receptor (SSTR)2 (ZA-0587; ZSGB-Bio; incubation for 40 minutes), and progesterone receptor (PR; M01879; Roche; incubation for 16 minutes) were used; (4) adding secondary antibody: after washing, add secondary antibody (FLEX/HRP; Agilent), incubate for 20 minutes, and wash for 5 minutes using the buffer; (5) DAB color rendering (FLEX DAB+Subchromo); and (6) hematoxylin and eosin staining of cell nucleus.

As for the IHC interpretation standards, by positive cell membrane staining showed EMA positivity; positive staining in the nucleus or cytoplasm, S-100 positivity; positive staining in the nucleus, PR positivity; and positive staining in the cytoplasm, vimentin positivity. For SSTR, negativity was no staining; +, at least 10% of tumor cells with weak cell membrane staining; ++, at least 10% of tumor cells with weak to moderate intensity of membrane staining; and +++, at least 10% of tumor cells with strong membrane staining.

Results

Clinical and Follow-up Information

In our PUMCH-MPMN cohort, most patients were females (86.4%; 76/88; *P* = 4.476 × 10⁻¹²). The average age was 58.9 years,

Table 1
Clinical features of 88 patients with MPMNs

Clinical features	Percentage (n/N)
Sex	
Male	13.6 (12/88)
Female	86.4 (76/88)
Age (y)	
Mean	58.9
Range	25-79
Smoking history	
Present/former	14.5 (10/69)
Never	85.5 (59/69)
No. of detected MPMNs	
Mean	1.52
Range	1-15
Location	
RUL	23.1 (31/134)
RML	3.0 (4/134)
RLL	32.1 (43/134)
LUL	14.9 (20/134)
LLL	26.9 (36/134)
Patient source	
Hospitalized surgical patients	78.4 (69/88)
Outpatient patients	21.6 (19/88)
Multiple primary lung cancer	
Yes	21.6 (19/88)
Average No. of lesions	3.9 (2-11)
Follow-up	
Survival and no progress	100.0 (69/69)

LLL, left lower lobe; LUL, left upper lobe; MPMN, minute pulmonary meningothelial-like nodule; RLL, right lower lobe; RML, right middle lobe; RUL, right upper lobe.

with a minimum age of 25 years. Similar to the characteristics of patients with MPLCs,^{19,20} most patients (85.5%, 59/69) had no smoking history, and most patients with MPMN with smoking were males. Each patient had an average of 1.52 MPMNs. We found only 1 MPMN in most patients (86.4%, 76/88), and identified a maximum of 15 MPMNs from 1 patient in our cohort. Unlike previous research,¹⁵ we found that MPMNs had lobe preferences in our cohort. MPMNs significantly tend to occur in the lower lobe (79/134; *P* = .01907) and right lungs (79/134; *P* = .02868). We collected follow-up imaging information for all 69 hospitalized patients. All patients survived, and no recurrence of MPMNs occurred after resection. Only 2 patients had suspected recurrence of their other tumor lesions. This was consistent with the benign characteristics of MPMNs. The clinical characteristics of these patients are demonstrated in Table 1.

Radiologic Characteristics of Minute Pulmonary Meningothelial-Like Nodules

CT is currently the most commonly used radiologic screening method for lung cancer. In our PUMCH-MPMN cohort, 50.7% (35/69) of MPMNs were visible on CT images (Table 2), similar to previous studies.^{4,6} Furthermore, among the MPMNs visible in imaging, the sizes of around half of them (57.1%, 20/35) were reported in CT reports. The diameter of these MPMNs ranged from 2.0 to 12.0 mm, with an average of 5.9 mm. This was similar to the average diameter reported by Wen et al⁶ (5.3 mm) and much larger than the average diameter reported by Mizutani et al¹⁵. The remaining nodules with sizes not reported independently were mainly reported as multiple tiny nodular opacities at corresponding locations.

Table 2
Radiologic features of MPMNs (69 patients)

Radiologic features	Percentage (n/N)
Visibility in CT images	
Visible	50.7 (35/69)
Enough size to be reported	57.1 (20/35)
Average size (mm)	5.9 (2 - 12)
Size not reported	42.9 (15/35)
Invisible	49.3 (34/69)
Appearance	
Pure GGO	40.0 (14/35)
Mixed GGO	8.6 (3/35)
Tiny nodular opacity	48.6 (17/35)
Solid nodule	2.9 (1/35)
PET/CT	
With PET/CT results and MPMN reported	20.3 (14/69)
No increase in radioactive uptake	92.9 (13/14)
Mild increase in radioactive uptake	4.9 (1/14)

CT, computed tomography; GGO, ground-glass opacity; MPMN, minute pulmonary meningothelial-like nodule; PET, positron emission tomography.

In terms of radiologic manifestations of MPMNs, most MPMNs were found as pure GGOs (40.0%, 14/35) and tiny nodular opacities (48.6%, 17/35) adjacent to the pleura on CT (Fig. 1A; Table 2). A few MPMNs also exhibited mixed GGO (8.6%, 3/35) and solid nodules (2.9%, 1/35). In addition, MPMNs exhibiting pure GGOs were accompanied by central vacuolar signs in 2 cases. Positron emission tomography/computed tomography (PET/CT) is often used to distinguish between benign and malignant lung lesions. In 20.3% (14/69) of patients, the radioactive uptake of MPMNs was reported based on PET/CT (Table 2). In 13 (92.9%) of these 14 patients, MPMNs were not observed with an increase in radioactive uptake, and the MPMN in the remaining patient (4.9%) was found with a mild rise in radioactive uptake. The SUV_{max} (standardized uptake value) of the MPMN in this patient was 1.4. Peng et al.⁴ reported that MPMN might increase metabolic uptake in PET/CT, with SUV_{max} reaching 4.8.⁴ However, this phenomenon was not observed in our cohort, and PET/CT can still effectively distinguish MPMNs from malignant nodules.

Histologic and Immunohistochemical Characteristics of Minute Pulmonary Meningothelial-Like Nodules

Under hematoxylin–eosin staining of MPMNs, meningothelial-like cells were arranged in nests or whorls with few stromal components. Higher-power magnification showed that the cells were always of medium size, with a round or oval nucleus, without any atypia or mitotic appearance (Fig. 1B). Sometimes, intranuclear inclusions and unclear cellular boundaries were observed.

MPMN are often found to exhibit IHC characteristics similar to meningiomas. In our cohort, 32 MPMNs from 20 patients were confirmed by IHC. These MPMNs were independent large lesions that required a clearer diagnosis. Table 3 and Supplementary Table summarize the IHC results of these MPMNs, including the positivity percentage and detection percentage of each marker. EMA, PR, and vimentin are 3 IHC staining markers for MPMNs with the broadest application,^{4,6,21–23} and they were positive in almost all MPMNs (Fig. 1C; Table 3). The high positivity rate of PR in the nuclei indicated that the growth of lesions may be related to hormones, explaining their higher incidence in females. Vimentin, a mesenchymal tissue marker, and EMA, an epithelial marker, showed positive results in the cytoplasm of almost all MPMNs,

also indicating the complex origin of MPMNs (Fig. 1C). Thyroid transcription factor (TTF)-1, as a pulmonary epithelial marker, is always used for exclusion diagnosis of MPMNs. However, in this study, there were also some MPMNs with TTF-1 positivity (25.9%) (Table 3). In recent years, some new meningioma biomarkers, such as SSTR2, have been found to be positive in MPMNs. In our cohort, 65.6% (21/32) of MPMNs measured SSTR2, and 20 of the 21 MPMNs were reported with SSTR2 positivity (Table 3). In addition, there were many biomarkers widely used for exclusion diagnosis of MPMNs in our cohort, including Ki-67 index, estrogen receptor, cytokeratin AE1/AE3, neuroendocrine tumor markers (S-100 and synaptophysin), melanoma markers (human melanoma black 45), and mesenchymal tissue markers (smooth muscle actin) (Table 3 and Supplementary Table).

Different Clinical Pathways for Finding Minute Pulmonary Meningothelial-Like Nodules

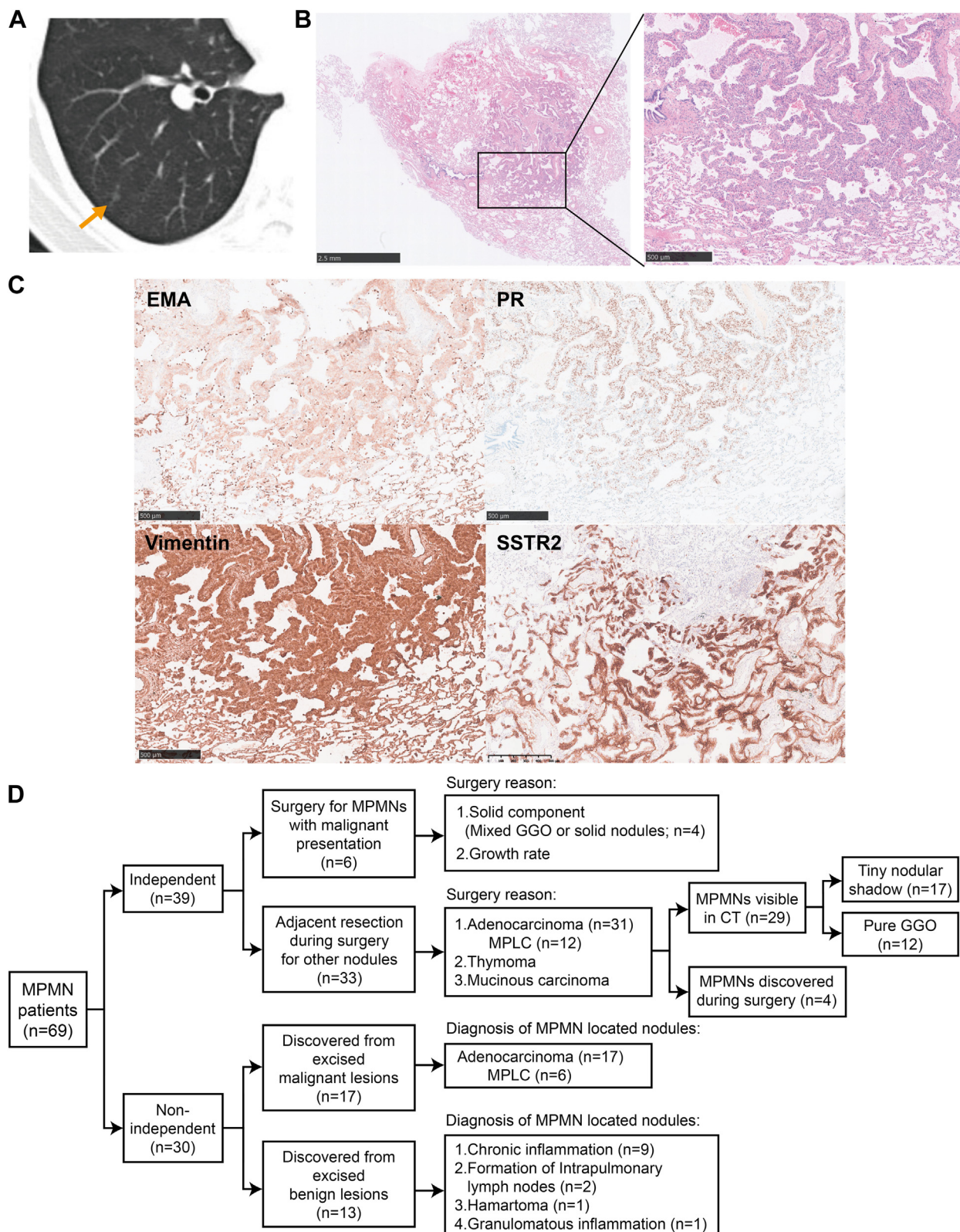
In clinical practice, MPMNs can be categorized into 2 distinct types: independent MPMNs, which are often misidentified as malignant lesions and surgically removed, and nonindependent MPMNs, incidentally detected in the peritumoral tissue. These 2 types hold different clinical significance. Based on radiologic and clinical characteristics, we propose a classification of MPMN discovery pathways into 4 distinct categories (Fig. 1D; Table 4): surgery for MPMNs with malignant presentation (8.7%, 6/69), independent lesions and adjacently resected during surgery for other nodules (47.8%, 33/69), discovered from excised malignant lesions (24.6%, 17/69), and discovered from excised benign lesions (18.8%, 13/69).

In patients who underwent surgery for independent MPMNs with radiologic features suggestive of malignancy, all detected MPMNs exceeded 7.0 mm in diameter on CT imaging, with solid components observed in 4 cases. Additionally, some lesions exhibited high growth rates. These malignant radiologic characteristics were the primary indications for surgical intervention (Fig. 1D). In rare cases, other surgical indications were observed. For instance, 1 patient underwent lung surgery to identify the source of ectopic adrenocorticotrophic hormone syndrome following multiple unsuccessful diagnostic attempts. The excised lesion was ultimately confirmed to be an MPMN.

Considering the widespread attention paid to MPLCs, more and more surgeons and patients choose to remove multiple lesions in 1 surgery, and adjacent resection during surgery for other nodules occupies an increasing proportion in finding MPMN pathways. In this pathway, most patients were diagnosed with adenocarcinoma (31/33), and 38.7% (12/31) were MPLCs. These MPMNs are mostly visible in CT (29/33) but with less-malignant CT appearances (tiny nodular shadow or pure GGO) (Fig. 1D). Patients with MPLC also had a greater number of MPMNs (2.6 MPMNs per patient) than other patients (1.3 MPMNs per patient), although this did not reach statistical significance ($P = .189$). As for nonindependent MPMNs, MPMNs were found in adenocarcinoma ($n = 17$), chronic inflammation ($n = 9$), formation of intra-pulmonary lymph nodes ($n = 2$), hamartoma ($n = 1$), or granulomatous inflammation ($n = 1$).

Whole-Exome Sequencing Revealing the Mutational Landscape of Minute Pulmonary Meningothelial-Like Nodules

We further conducted WES in 12 MPMNs and 7 simultaneously removed multiple primary adenocarcinoma lesions from 6

**Figure 1.**

Clinical, pathologic, and radiologic features of MPMNs. (A) CT images of MPMNs. The MPMN was observed as a pure ground-glass opacity (GGO). (B) Hematoxylin-and-eosin-stained pathologic images. Short spindle-shaped cells were found with nest-like arrangements in the MPMN, with few stromal components and without any atypia or mitotic appearance. (C) Immunohistochemical images of MPMNs. PR (in the nuclei), EMA, Vimentin, and SSTR2 (in the cytoplasm) are found to be positive. (D) Different clinical pathways of finding MPMNs, demonstrating the MPMNs discovered through 4 different ways, as well as the surgery reasons and clinical diagnosis. CT, computed tomography; EMA, epithelial membrane antigen; MPLC, multiple primary lung cancer; MPMN, minute pulmonary meningotheelial-like nodule; PR, progesterone receptor.

Table 3
Immunohistochemical features of MPMNs

Immunohistochemical markers	Positivity percentage (n/N)
EMA	96.8 (30/31)
PR	90.6 (29/32)
Vimentin	100.0 (28/28)
SSTR2	95.2 (20/21)
TTF-1	25.9 (7/27)
Ki-67 index	10.5 (index > 1, 2/19)
AE1/AE3	12.5 (2/16)
S-100	6.3 (1/16)
SMA	6.7 (1/15)
HMB45	14.3 (2/14)
ER	0.0 (0/11)
Synaptophysin	0.0 (0/9)

EMA, epithelial membrane antigen; ER, estrogen receptor; HMB, human melanoma black; MPMN, minute pulmonary meningothelial-like nodule; PR, progesterone receptor; SSTR, somatostatin receptor type; SMA, smooth muscle actin; TTF, thyroid transcription factor.

patients. These MPMNs were all independent lesions, and their diagnosis were confirmed by pathologists. In these MPMNs, we did not find classical mutations of meningiomas, such as *NF2*, *TRAF7*, *AKT1*, *KLF4*, and *TERT* mutations^{24–28} (Fig. 2A–C). This supports the differential origin of MPMNs and meningiomas. Moreover, based on the phylogenetic trees of lesions from each patient, we found that there were almost no shared mutations among MPMNs, as well as between MPMNs and malignant lesions (Fig. 2D), further confirming the independent origin of each MPMN. Furthermore, we detected mutations in multiple genes related to the cell cycle and corresponding signal transduction pathways (Fig. 2A–C, E, F), such as *BRAF*, *NFIC* (nuclear factor I C), *CDC25C* (cell division cycle 25C), *PTPRT* (protein tyrosine phosphatase receptor type T), *PPP2R3B* (protein phosphatase 2 regulatory subunit B). The mutated genes were also found enriched in some cytoskeleton or muscle-related gene ontology terms like actin filament organization and stress fiber assembly (Fig. 2D), suggesting the relationships between MPMN mutations and actin

filament formation changes, which may be one of the reasons why MPMNs form a unique histologic morphology.

Considering mutations in pathways related to cell proliferation and the high incidence of MPMNs in patients with chronic lung diseases, we speculated that reactive hyperplasia is the main cause of MPMNs. Somatic mutations still participate in excessive cell proliferation in MPMNs, but the lack of shared mutations also indicates that there may be no fixed pathway for early proliferation in MPMNs. In other words, the growth of MPMNs could be not driven by meningioma-related mechanisms. The meningioma-like histologic characteristics, including the high positivity rate of SSTR2, could result from reactive hyperplasia or a manifestation of the late growth stage.

Discussion

MPMN are rare, benign pulmonary lesions that can be misdiagnosed due to their radiologic resemblance to malignant nodules. Their distinct histologic features and uncertain etiology have garnered significant interest among surgeons and pathologists. In the study, we collected data from patients with MPMN diagnosis from Peking Union Medical College Hospital in the past 5 years. Our PUMCH-MPMN cohort included 88 patients with 134 MPMNs in total. To the best of our knowledge, we provided the first WES results of MPMNs, providing new evidence for the origin of MPMN. Summarizing the 4 types of MPMNs with different finding ways, we also found a large proportion of independent MPMNs adjacently resected during surgery for other nodules, especially during the surgery for MPLC.

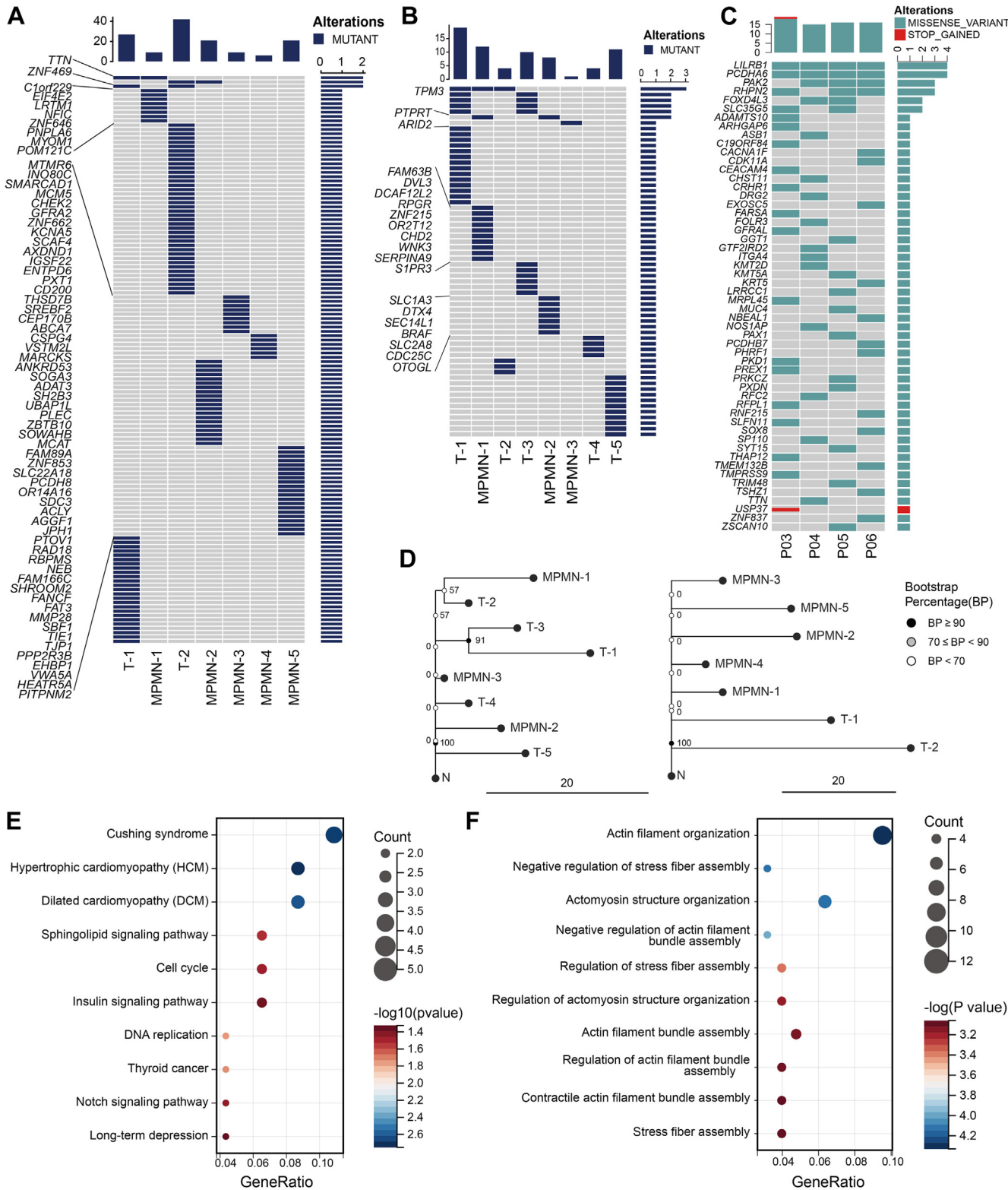
Regarding the pathologic characteristics of MPMNs, we calculated the detection and positivity percentages of various IHC markers in MPMN. Our results further support the good performance of SSTR2 in diagnosis.²² We also verified the diagnostic value of the 3 classic MPMN diagnostic markers (EMA, PR, and vimentin), and the exclusion diagnosis value of classic estrogen receptor, AE1/AE3, neuroendocrine tumor markers (S-100 and synaptophysin), melanoma markers (human melanoma black 45), mesenchymal tissue markers (smooth muscle actin). Unlike other studies,^{4,6} we also found some MPMNs with positivity in TTF-1 staining, indicating MPMNs with proliferation ability and characteristics similar to lung epithelium. In addition, based on literature research, we also discovered some new markers, such as insulinoma-associated protein 1,²³ which can be applied to the pathologic diagnosis of MPMNs in the future.

As for the clinical and radiologic characteristics of MPMNs, MPMNs are indeed found with some malignant CT manifestations, such as solid components and vacuolar signs, and other malignant manifestations have also been reported in the literature.^{29,30} These malignant presentations in CT are always the surgical causes of the first type of MPMNs in our classification criteria. However, our results indicate that PET/CT still has good differential diagnostic value for MPMNs. PET/CT examination or other advanced imaging tests³¹ for suspicious lesions can help some patients avoid surgery or reduce the number of excised nodules, preserving more lung function. After MPLC gradually gained attention, the second type of MPMNs, which was independent and adjacently resected during surgery for other nodules, accounted for nearly half of the proportion of MPMNs. Especially considering that these lesions are often not in the same lung lobe, strict judgment, effective preoperative examination methods, and soothing patient anxiety are necessary.

Table 4
Diagnosis of patients with MPMNs

Diagnosis information	Percentage (n/N)
Reasons of surgical decision	
Independent MPMNs with malignant presentation	8.7 (6/69)
Independent MPMNs with a low possibility of malignancy, adjacent resection during surgery for other nodules	47.8 (33/69)
Nonindependent MPMNs, discovered from excised malignant lesions	24.6 (17/69)
Nonindependent MPMNs, discovered from excised benign lesions	18.8 (13/69)
Main patient diagnosis	
Adenocarcinoma	65.9 (58/88)
AAH	5.7 (5/88)
AIS	11.4 (10/88)
MIA	19.3 (17/88)
IAC	29.5 (26/88)
MPMN	11.4 (10/88)
Chronic inflammation or immune cell infiltrating nodules	9.1 (8/88)
Hamartoma	2.3 (2/88)
Others	11.4 (10/88)

AAH, atypical adenomatoid hyperplasia; AIS, adenocarcinoma in situ; IAC, invasive adenocarcinoma; MIA, minimally invasive adenocarcinoma; MPMN, minute pulmonary meningothelial-like nodule.

**Figure 2.**

The mutational landscape of MPMNs revealed by WES. (A,B) Heatmaps showed the presence (blue) or absence (gray) of somatic mutations. Samples include tumors (T) and MPMNs from 2 patients. (C) Heatmaps showed the presence (blue) or absence (gray) of somatic mutations in 4 patients with single MPMNs. (D) Phylogenetic trees indicated the clonal structure of lesions in each patient. (E) Kyoto Encyclopedia of Genes and Genomes enrichment analyses on mutated genes. (F) Gene ontology enrichment analyses (biological process module) on mutated genes. MPMN, minute pulmonary meningothelial-like nodule.

The pathogenesis of MPMN has not yet reached a consensus. There has been controversy over whether MPMNs are reactive hyperplasia or share mechanisms with central nervous system meningioma. Previous research has provided some evidence for both hypotheses. Ionescu et al¹¹ analyzed loss of heterozygosity (LOH) events in MPMNs and meningiomas. They found that MPMNs rarely exhibit more than 1 LOH, whereas meningiomas exhibit high-frequency LOH, and common LOH (22q, 14q, and 1p) of meningiomas cannot be observed in MPMNs, suggesting that MPMNs have a reactive origin. In addition, they found that multiple LOH is seen only in diffuse pulmonary meningiomatosis (DPM), suggesting that DPM may be a transition between reactive proliferation and tumorigenic proliferation.¹¹ In addition, Niho et al³² analyzed the clonality of MPMNs using methylation-sensitive restriction endonucleases. Among the 11 lesions, 5 were derived from polyclonal amplification and 6 from monoclonal amplification, and there was no histologic difference between the monoclonal and polyclonal MPMNs. Thus, they believed that MPMNs may be a source of reactive proliferation rather than tumors. On the contrary, some studies also suggest that MPMNs share mechanisms with central nervous system meningiomas. MPMNs have pathologic characteristics similar to primary and metastatic pulmonary meningiomas and can be classified together as pleuropulmonary meningeal proliferation.^{7,14} At the molecular level, neurofibromatosis type 2 (NF2) gene deletions in 22q are common in meningiomas. Weissferdt et al¹⁴ found NF2 deletions in some MPMNs (2/6) through fluorescence in situ hybridization, suggesting that MPMNs and meningiomas have similar origins and common molecular pathways.

Based on the WES results in our PUMCH-MPMN cohort, we did not find classical mutations of meningiomas. Compared with other mutation detection technologies, the sufficient coverage and sequencing depth of WES provide a mutation landscape of MPMNs. Based on WES results, we speculated the mutation in MPMNs enriched in cell-cycle signal transduction and cytoskeleton-related pathways. Moreover, these MPMNs had no histologic differences, but there were nearly no common mutations among them, indicating that these similar MPMNs could have different growth mechanisms. These findings all support the reactive hyperplasia theory. We also propose that the reactive proliferation and meningioma-related molecular pathways may not be contradictory. MPMNs may originate from reactive proliferation in the early stages. Subpleural stromal multipotent mesenchymal cells and dispersed ectopic arachnoid rest cells during embryonic development may serve as the primitive cells of MPMNs.¹⁴ In the later stage of MPMN development, these primitive cells transdifferentiate into cells similar to the meningeal epithelium, causing the meningioma-like histologic characteristics of MPMNs. MPMNs may contain both cells in the early reactive proliferation stage and cells with late meningioma-like growth. In the future, we will further explore the pathogenesis of MPMNs through single-cell genomics and single-cell transcriptomics analysis.³³⁻³⁵ Further, we will collect DPM or primary pulmonary meningiomas with large masses and conduct WES to verify this hypothesis.

As for the limitation of our study, first, owing to the small size and rarity of MPMNs, there were not many high-quality fresh MPMN samples for WES and the number of MPMNs included in WES in this study was relatively small. We will continue to collect MPMN cases to expand the cohort and collect more WES results in order to obtain a more comprehensive mutation spectrum of MPMNs in the population. Second, this study did not involve experimental verification or mechanism research. The exact pathogenesis of MPMNs still needs to be confirmed by

experiments. We will further explore the construction of MPMN models and observe whether the introduction of mutations can lead to the appearance of MPMN in model animals. In addition, the population included in this study was mainly Asians. Considering that Asians account for the majority of patients in our hospital, we will collaborate with hospitals in other countries in the future to collect clinical and mutation information on MPMNs of other ethnic groups to reduce racial bias.

In summary, our study provided new evidence that MPMNs originate from reactive proliferation. We emphasized the significance of PET/CT and new IHC markers in the screening and diagnosis of MPMNs. Our research contributes to a deeper understanding of the response mechanism of the lungs to chronic diseases such as tumors. It can also help clinicians and pathologists gain a deeper understanding of such lesions, increase the radiologic and pathologic diagnosis rates of MPMNs, and reduce patient harm.

Acknowledgments

The authors thank the Clinical Biobank (ISO 20387) at Peking Union Medical College Hospital, Chinese Academy of Medical Sciences, for their assistance in sample collection.

Author Contributions

H.L., Z.H., Y.W., C.G., X.L., S.W., N.B., H.C., B.L., D.W., Z.Z., Z.B., Y.S., Y.X., G.H., and K.F.: substantial contributions to the conception or design of the work or the acquisition, analysis, or interpretation of data for the work. H.L., N.L., and S.L.: drafting the work or reviewing it critically for important intellectual content. N.L. and S.L.: final approval of the version to be published. N.L. and S.L.: agreement to be accountable for all aspects of the work.

Data Availability

Data are available upon reasonable request.

Funding

This work was supported by the National High-Level Hospital Clinical Research Funding (2022-PUMCH-B-011 and 2022-PUMCH-A-106) and Beijing Xisike Clinical Oncology Research Foundation (CSCO-Y-MSDPU2021-0190).

Declaration of Competing Interest

S. Wang, N. Bai, and H. Chen are employees of Nanjing Geneeq Technology Inc. The remaining authors declare no competing interests.

Ethics Approval/Consent to Participate

This study involved human participants and was approved by the ethical committee of Peking Union Medical College Hospital (K7403). All patients have signed written informed consent forms for genomic profiling.

Supplementary Material

The online version contains supplementary material available at <https://doi.org/10.1016/j.labinv.2025.104188>

References

1. Korn D, Bensch K, Liebow AA, Castleman B. Multiple minute pulmonary tumors resembling chemodectomas. *Am J Pathol*. 1960;37(6):641–672.
2. Gaffey MJ, Mills SE, Askin FB. Minute pulmonary meningotheelial-like nodules. A clinicopathologic study of so-called minute pulmonary chemodectoma. *Am J Surg Pathol*. 1988;12(3):167–175. <https://doi.org/10.1097/00000478-198803000-00001>
3. Churg AM, Warnock ML. So-called “minute pulmonary chemodectoma”: a tumor not related to paragangliomas. *Cancer*. 1976;37(4):1759–1769. [https://doi.org/10.1002/1097-0142\(197604\)37:4<1759::aid-cncr282037042>3.0.co;2-3](https://doi.org/10.1002/1097-0142(197604)37:4<1759::aid-cncr282037042>3.0.co;2-3)
4. Peng XX, Yan LX, Liu C, et al. Benign disease prone to be misdiagnosed as malignant pulmonary nodules: minute meningotheelial nodules. *Thorac Cancer*. 2019;10(5):1182–1187. <https://doi.org/10.1111/1759-7714.13061>
5. Goldblum JR, Lamps LW, McKenney JK. *Rosai and Ackerman's Surgical Pathology*. 11th ed. Elsevier Health Sciences; 2017.
6. Wen Z, Zhang Y, Fu F, et al. Clinical, pathological and radiologic features of minute pulmonary meningotheelial-like nodules. *J Cancer Res Clin Oncol*. 2022;148(6):1473–1479. <https://doi.org/10.1007/s00432-021-03744-x>
7. Lin D, Yu Y, Wang H, et al. Radiological manifestations, histological features and surgical outcomes of pulmonary meningotheelial proliferation: a case series and rethinking. *Transl Lung Cancer Res*. 2020;9(4):1159–1168. <https://doi.org/10.21037/tlc-19-699>
8. Masago K, Hosada W, Sasaki E, et al. Is primary pulmonary meningioma a giant form of a meningotheelial-like nodule? A case report and review of the literature. *Case Rep Oncol*. 2012;5:471–478. <https://doi.org/10.1159/000342391>
9. Bernabeu Mora R, Sánchez Nieto JM, Hu C, Alcaraz Mateos E, Giménez Bascuñana A, Rodríguez Rodríguez M. Diffuse pulmonary meningotheiomatosis diagnosed by transbronchial lung biopsy. *Respiration*. 2013;86(2):145–148. <https://doi.org/10.1159/000350430>
10. Suster S, Moran CA. Diffuse pulmonary meningotheiomatosis. *Am J Surg Pathol*. 2007;31(4):624–631. <https://doi.org/10.1097/01.pas.0000213385.25042.cfm>
11. Ionescu DN, Sasatomi E, Aldeeb D, et al. Pulmonary meningotheelial-like nodules: a genotypic comparison with meningiomas. *Am J Surg Pathol*. 2004;28(2):207–214. <https://doi.org/10.1097/00000478-200402000-00008>
12. Li H, Xue J, Li P, et al. [Recent advances and controversies in minute pulmonary meningotheelial-like nodules]. *Zhongguo Fei Ai Za Zhi*. 2023;26(8):621–629. <https://doi.org/10.3779/j.issn.1009-3419.2023.102.30>
13. Mukhopadhyay S, El-Zammar OA, Katzenstein ALA. Pulmonary meningotheelial-like nodules: new insights into a common but poorly understood entity. *Am J Surg Pathol*. 2009;33(4):487–495. <https://doi.org/10.1097/PAS.0b013e31818b1de7>
14. Weissferdt A, Tang X, Suster S, Wistuba II, Moran CA. Pleuropulmonary meningotheelial proliferations: evidence for a common histogenesis. *Am J Surg Pathol*. 2015;39(12):1673–1678. <https://doi.org/10.1097/PAS.0000000000000489>
15. Mizutani E, Tsuta K, Maeshima AM, Asamura H, Matsuno Y. Minute pulmonary meningotheelial-like nodules: clinicopathologic analysis of 121 patients. *Hum Pathol*. 2009;40(5):678–682. <https://doi.org/10.1016/j.humpath.2008.08.018>
16. Fang W, Ma Y, Yin JC, et al. Comprehensive genomic profiling identifies novel genetic predictors of response to anti-PD-(L)1 therapies in non-small cell lung cancer. *Clin Cancer Res*. 2019;25:5015–5026. <https://doi.org/10.1158/1078-0432.CCR-19-0585>
17. Lai Z, Markovets A, Ahdesmaki M, et al. VarDict: A novel and versatile variant caller for next-generation sequencing in cancer research. *Nucleic Acids Res*. 2016;44:e108. <https://doi.org/10.1093/nar/gkw227>
18. Niknafs N, Beleva-Guthrie V, Naiman DQ, Karchin R. SubClonal hierarchy inference from somatic mutations: automatic reconstruction of cancer evolutionary trees from multi-region next generation sequencing. *PLoS Comput Biol*. 2015;11:e1004416. <https://doi.org/10.1371/journal.pcbi.1004416>
19. Wang Y, Huang Z, Li B, et al. Clonal expansion of shared T cell receptors reveals the existence of immune commonality among different lesions of synchronous multiple primary lung cancer. *Cancer Immunol Immunother*. 2024;73(6):111. <https://doi.org/10.1007/s00262-024-03703-8>
20. Li H, Huang Z, Guo C, et al. Super multiple primary lung cancers harbor high-frequency BRAF and low-frequency EGFR mutations in the MAPK pathway. *NPJ Precis Oncol*. 2024;8(1):229. <https://doi.org/10.1038/s41698-024-00726-3>
21. Zhang Y, Wu J, Zhang T, Zhang Q, Chen YC. Minute pulmonary meningotheelial-like nodules: Rare lesions appearing as diffuse ground-glass nodules with cyst-like morphology. *Quant Imaging Med Surg*. 2021;11(7):3355–3359. <https://doi.org/10.21037/qims-20-676>
22. Tao L, Chen Y, Huang Q, Yong J, Yan S, Huang Y. Constant expression of somatostatin receptor 2a in minute pulmonary meningotheelial-like nodules. *J Clin Pathol*. 2019;72(8):525–528. <https://doi.org/10.1136/jclinpath-2019-205913>
23. Dermawan JK, Mukhopadhyay S. Insulinoma-associated protein 1 (INSM1) differentiates carcinoid tumourlets of the lung from pulmonary meningotheelial-like nodules. *Histopathology*. 2018;72(6):1067–1069. <https://doi.org/10.1111/his.13458>
24. Pellerino A, Bruno F, Palmiero R, et al. Clinical significance of molecular alterations and systemic therapy for meningiomas: where do we stand? *Cancers (Basel)*. 2022;14:2256. <https://doi.org/10.3390/cancers14092256>
25. Mawrin C, Perry A. Pathological classification and molecular genetics of meningiomas. *J Neurooncol*. 2010;99:379–391. <https://doi.org/10.1007/s11060-010-0342-2>
26. Clark VE, Erson-Omay EZ, Serin A, et al. Genomic analysis of non-NF2 meningiomas reveals mutations in TRAF7, KLF4, AKT1, and SMO. *Science*. 2013;339:1077–1080. <https://doi.org/10.1126/science.1233009>
27. Abedalthagafi M, Bi WL, Aizer AA, et al. Oncogenic PI3K mutations are as common as AKT1 and SMO mutations in meningioma. *Neuro Oncol*. 2016;18:649–655. <https://doi.org/10.1093/neuonc/nov316>
28. Reuss DE, Piro RM, Jones DTW, et al. Secretory meningiomas are defined by combined KLF4-K409Q and TRAF7 mutations. *Acta Neuropathol*. 2013;125:351–358. <https://doi.org/10.1007/s00401-013-1093-x>
29. Harada M, Aono Y, Yasui H, et al. Minute pulmonary meningotheelial-like nodules showing multiple ring-shaped opacities. *Intern Med*. 2019;58(21):3149–3152. <https://doi.org/10.2169/internalmedicine.2108-18>
30. Kraushaar G, Ajlan AM, English JC, Müller NL. Minute pulmonary meningotheelial-like nodules: a case of incidentally detected diffuse cystic micronodules on thin-section computed tomography. *J Comput Assist Tomogr*. 2010;34(5):780–782. <https://doi.org/10.1097/RCT.0b013e3181e47c28>
31. Wang J, Huang Z, Zhu Z, et al. Photon-counting detector CT provides superior subsolid nodule characterization compared to same-day energy-integrating detector CT. *Eur Radiol*. Published online November 28, 2024. <https://doi.org/10.1007/s00330-024-11204-6>
32. Niho S, Yokose T, Nishiwaki Y, Mukai K. Immunohistochemical and clonal analysis of minute pulmonary meningotheelial-like nodules. *Hum Pathol*. 1999;30(4):425–429. [https://doi.org/10.1016/S0046-8177\(99\)90118-1](https://doi.org/10.1016/S0046-8177(99)90118-1)
33. Li H, Ma T, Zhao Z, et al. scTML: a pan-cancer single-cell landscape of multiple mutation types. *Nucleic Acids Res*. 2025;53(D1):D1547–D1556. <https://doi.org/10.1093/nar/gkae898>
34. Xi X, Li H, Chen S, et al. Unfolding the genotype-to-phenotype black box of cardiovascular diseases through cross-scale modeling. *iScience*. 2022;25:104790. <https://doi.org/10.1016/j.isci.2022.104790>
35. Ma T, Li H, Zhang X. Discovering single-cell eQTLs from scRNA-seq data only. *Gene*. 2022;829:146520. <https://doi.org/10.1016/j.gene.2022.146520>